Microparticles in a Collisional Rf Plasma Sheath under Hypergravity Conditions as Probes for the Electric Field Strength and the Particle Charge

J. Beckers,[1] T. Ockenga,[2] M. Wolter,[2] W. W. Stoffels,[1] J. van Dijk,[1] H. Kersten,[2] and G. M. W. Kroesen[1]

[1]*Eindhoven University of Technology, Department of Applied Physics P.O. Box 513, 5600 MB, Eindhoven, The Netherlands*
[2]*Institut für Experimentelle und Angewandte Physik, Christian-Albrechts-Universität Kiel,
Olshausenstraße 40-60, 24098 Kiel, Germany*

We used microparticles under hypergravity conditions, induced by a centrifuge, in order to measure nonintrusively and spatially resolved the electric field strength as well as the particle charge in the collisional rf plasma sheath. The measured electric field strengths demonstrate good agreement with the literature, while the particle charge shows decreasing values towards the electrode. We demonstrate that it is indeed possible to measure these important quantities without changing or disturbing the plasma.

1. INTRODUCTION.—When a quasineutral plasma is in contact with a solid surface, an electric space charge region—the plasma sheath—builds up near the surface due to the difference in mobility between the electrons and the much heavier ions. Understanding sheath phenomena is of major importance for almost all plasma applications where the acceleration of positive ions at the border of the discharge is involved (e.g., deposition, etching, and sputtering). Today, most processes in the plasma sheath are not fully understood as experimental data concerning plasma parameters in the sheath are extremely hard to obtain. Researchers have proposed many models to predict the electric field and potential profiles within the sheath [1–3]. Experimentally, electric fields in the sheath have been determined by means of Stark splitting [4] and Stark shift [5,6]. Another method to investigate the sheath region experimentally is based on phase-resolved probe measurements [7]. However, those measurements severely disturb the local electric field. In 2005, Samarian *et al.* [8] introduced plasma-confined microparticles as electrostatic probes in the rf sheath. Later, this method was extended for confined particles in a tailored sheath in front of an adaptive electrode [9]. The resonance of particles in the sheath has been extensively studied by Zafiu *et al.* [10]. Until now, these experiments have all been performed at one particle position in the sheath: the position where the electrostatic force equilibrates gravity. Hence, a desired change in the particle position can only be achieved by either using particles with a different size, by changing the bias voltage, or by an additional ion flux [11]. These changes all severely disturb plasma conditions in the experiment.

In this Letter we demonstrate that it is indeed possible to measure the electric field structure and the charge of microparticles at any position in the plasma sheath, nonintrusively, without the plasma being changed or disturbed. An additional nonelectric force is introduced which does not alter the plasma conditions, but which does allow for manipulation of the particle position through the sheath:

(hyper-)gravity, induced by a centrifuge. By adjusting the apparent gravity, the equilibrium position of the microparticles is changed without further disturbance of the plasma. Consequently, the electric field and the particle charge can be determined using one and the same particle for measurements at several positions throughout the sheath. In addition to the obtained fundamental knowledge about the sheath and the great importance for the large range of plasma applications where acceleration of ions is utilized, knowledge about the particle charge can be of major interest for interpreting the many ongoing complex plasma experiments in the International Space Station [12–14].

2. THEORY.—

2.1. Sheath Model.—When a microparticle with constant mass m_p is in its equilibrium confinement position z_E in the sheath, the resultant force working on it is zero. Here, the positive z axis is directed along the gravitational acceleration vector and perpendicular to the electrodes. The sheath edge is at $z = 0$ and the rf electrode is at $z = \xi$, where ξ is the sheath width. From the measurements of the apparent gravitational acceleration g^*—induced by a centrifuge—necessary to force the particle in position z_E, we obtain the function $g^*(z_E)$ and, from that, we derive the time-averaged and spatially resolved electric field strength $E(z_E)$, the electric potential $\varphi(z_E)$, and the particle charge $Q_p(z_E)$ as follows.

The two dominant forces working on the stationary-confined microparticle are the electrostatic force $\vec{F}_E(z_E) = Q_p(z_E)\vec{E}(z_E)$ and the gravitational force $\vec{F}_g(z_E) = m_p\vec{g}^*(z_E)$. The plasma chamber is sealed during plasma operation (no neutral drag force) and due to the low plasma powers used, the plasma and its surroundings are assumed not to heat up significantly (negligible thermophoretic force). Basner *et al.* [9] already showed that ion drag forces at microparticles with sizes as used in our experiments are negligible with respect to $\vec{F}_E$ and $\vec{F}_g$. The force balance on the particle yields

$$Q_p(z_E)E(z_E) = m_p g^*(z_E), \qquad (1)$$

and in its differential form

$$E(z_E)\frac{dQ_p(z_E)}{dz_E} + Q_p\frac{dE(z_E)}{dz_E} = m_p\frac{dg^*(z_E)}{dz_E}. \qquad (2)$$

In general $E(z)$ and $\varphi(z)$ are related to the time-averaged space charge density $\rho(z)$ according to the Poisson equation. When the electron density n_e is assumed to be much smaller than the ion density n_i in almost the full sheath ($n_e \ll n_i$), and the ion flux Γ_i is assumed to be conserved throughout the sheath (no ionization), this Poisson equation reads

$$-\frac{d^2\varphi(z)}{dz^2} = \frac{dE(z)}{dz} = \frac{\rho(z)}{\varepsilon_0} \approx \frac{en_i(z)}{\varepsilon_0} = \frac{e\Gamma_{i,\mathrm{sh}}}{\varepsilon_0 v_i(z)}. \qquad (3)$$

Here, e is the electron charge, ε_0 the dielectric constant, $v_i(z)$ the ion velocity at position z and $\Gamma_{i,\mathrm{sh}} = n_{i,\mathrm{sh}}v_{i,\mathrm{sh}}$ the ion flux at the sheath edge with $n_{i,\mathrm{sh}}$ and $v_{i,\mathrm{sh}}$ the ion density and velocity at the sheath edge, respectively. Note that, although $n_e(z)$ does not contribute to $\rho(z)$, the electrons, periodically flooding the sheath during a small fraction of each rf cycle, are responsible (together with the ion flux towards the particle surface) for the negative charge and charging of the particle.

In order to describe the ion motion and, hence, $v_i(z)$ in Eq. (3), we must first determine whether the sheath has to be considered in either the collisionless regime, the collisional regime, or in the transition regime separating these. To do so, we compare the sheath width ($\xi = 7.0 \pm 0.5$ mm) with the ion mean-free path λ_{mfp}. The sheath width is determined by means of measuring the position at which the light emission is a factor $1/e$ of the light emission from the plasma bulk and its error from the positions where the emission intensity has values of 10% and 90% of the bulk emission. The ion mean-free path is given by $\lambda_{\mathrm{mfp}} = (n_n\sigma_{i-n})^{-1}$ with n_n the neutral gas density and $\sigma_{i-n} = 8 \times 10^{-19}$ m^2 the ion-neutral collision cross section, assumed independent of v_i [15]. For the pressure used in our experiments (20 Pa), $\lambda_{\mathrm{mfp}} = 0.26$ mm. Hence $\xi \gg \lambda_{\mathrm{mfp}}$ and the sheath is considered to be collisional. Neglecting ionization, the simplified fluid equation of motion for ions with mass M_i is given by

$$M_i v_i(z)\frac{dv_i(z)}{dz} = eE(z) - M_i\frac{v_i^2(z)}{\lambda_{\mathrm{mfp}}}. \qquad (4)$$

For our conditions ($\xi \gg \lambda_{\mathrm{mfp}}$ and $T_{\mathrm{ion}} \approx 300$ K), the inertia term on the left-hand side of Eq. (4) can safely be neglected [3], The ion velocity $v_i(z)$ is then given by $v_i(z) = \alpha\sqrt{E(z)}$, with $\alpha = (2e\lambda_{\mathrm{mfp}}/\pi M_i)^{1/2}$. This expression for $v_i(z)$ has been used before by several other researchers for collisional sheath models [1,15,16].

Combining this expression for $v_i(z)$ with the Poisson equation [Eq. (3)], substituting into Eq. (2), and eliminating

$E(z_E)$ by using Eq. (1) yields the following differential equation for $Q_p(z_E)$:

$$\frac{dQ_p(z_E)}{dz_E} = \frac{dg^*(z_E)}{dz_E}\frac{Q_p(z_E)}{g^*(z_E)} - \frac{\Gamma_{i,\mathrm{sh}}}{\alpha\varepsilon_0}\frac{eQ_p^{5/2}(z_E)}{(m_p g^*(z_E))^{3/2}}. \qquad (5)$$

When a proper boundary condition is chosen, Eq. (5) can be solved iteratively and consequently the spatial profiles for $Q_p(z_E)$, $E(z_E)$, and $\varphi(z_E)$ are obtained.

2.2. Boundary Conditions.—Since our lowest gravitational level is $1g_0$ (with $g_0 = 9.81$ m/s^2), no experimental data are available for $z_E < 1.67$ mm. Still, in order to be able to integrate Eq. (5), we need to specify a boundary value for E (and thus for Q_p) at $z_E = 1.67$ mm. This is done by approximating the sheath as a linear one for $0 < z_E < 1.67$ mm. The boundary value $E(z_E = 1.67$ mm) is now chosen such that, when the determined $\varphi(z_E)$ profile is extrapolated with a high-order polynomial function to the electrode, the value $\varphi_{\mathrm{fit}} = \varphi(z_E = \xi)$ matches the measured electrode bias potential φ_{bias}.

Crucial for determining the ion flux $\Gamma_{i,\mathrm{sh}}$ at the sheath edge is the value of the velocity with which the ions enter the sheath. A good estimate for this velocity is the Bohm velocity. Riemann showed that, although the sheath edge becomes more fuzzy for higher collisionalities, this estimate also holds in the case of a collisional sheath [17]. Accordingly, we have calculated the velocity of the ions at the sheath edge by $v_{i,\mathrm{sh}} = v_B = (eT_e/M_i)^{1/2}$, with T_e equaling the electron temperature.

3. EXPERIMENTAL SETUP AND PROCEDURE.—The experiments are performed in a cubic ($20 \times 20 \times 20$ cm^3) stainless steel vacuum chamber containing a capacitively coupled parallel plate rf argon discharge operated at 13.56 MHz and $\sim$5 W. The two 7×7 cm^2 squared electrodes are oriented in the horizontal plane and separated 4 cm from each other. The bottom electrode is rf driven and a copper ring is mounted on top in order to trap the inserted microparticles in its potential well. On top of the vacuum chamber, a computer-controlled dust dispenser is mounted, injecting monodisperse melamine formaldehyde particles with diameters of 10.2 μm into the plasma volume. The whole chamber is mounted onto a centrifuge. A gondola, which is mounted at the end of one arm, is able to swing outwards when the centrifuge rotates, directing the resulting apparent gravitational force perpendicular to its ground plate. The maximum apparent gravitational force that can be achieved at the position of the ground plate of the gondola is $10g_0$. On top of the centrifuge arm, two function generators, an rf power amplifier and a match box are mounted. The function generators are operated by a computer, allowing for rf power modulation in order to perform particle resonance measurements. A mobile pumping and gas supply system is used to pump down the vacuum chamber and fill it with argon up to a pressure of 20 Pa. An expanded 532 nm laser beam illuminates the particles which are photographed at an angle of 90° with the laser
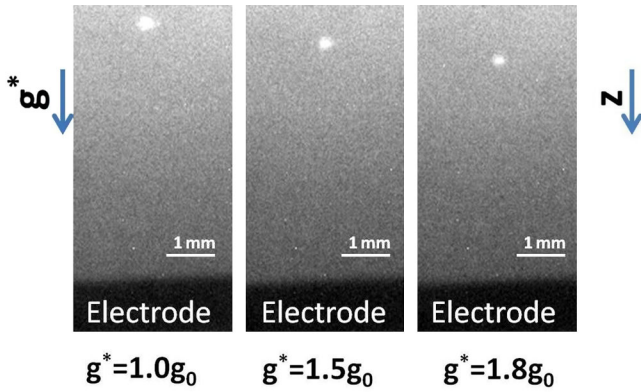
FIG. 1 (color online).   CCD camera images of a microparticle, confined within the plasma sheath under several hyper-gravity conditions.

beam by an on-board CCD camera. A computer, mounted in the centrifuge gondola, has a wireless connection with the operating computer in the centrifuge control room. Via this connection, the dust dispenser, the function generators, and the CCD camera can be remote controlled while the centrifuge rotates.

The plasma potential φ_{pl} and the plasma density ($n_{e,0} = n_{i,0}$) in the middle of the discharge have been determined by means of passively compensated Langmuir probe measurements, The probe tip was a 3 mm-long tungsten wire with a diameter of 10 μm. φ_{pl} is obtained from the point at which the first derivative of the probe characteristic is zero and the electron density from the ion saturation current. The results yield $\varphi_{pl} = 32$ V and $n_{e,0} = 7.0 \times 10^{14}$ m^{-3}, with an estimated error of 20%. The electrode bias potential ($\varphi_{bias} = -82 \pm 1$ V) has been measured with a commercial plasma impedance monitor (SmartPIM) of Scientific Systems.
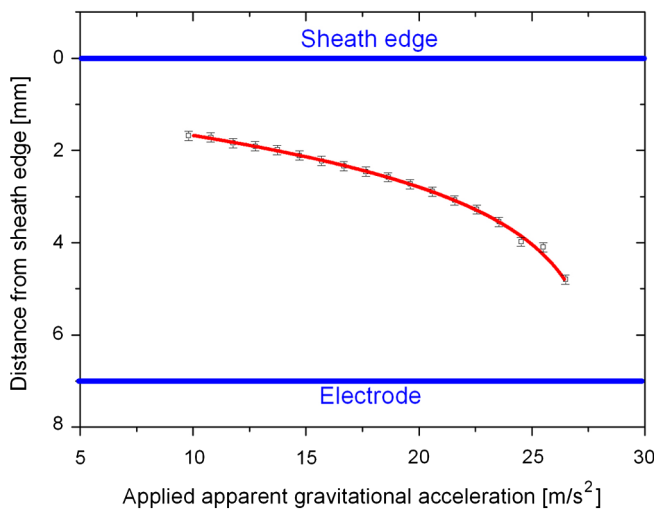
FIG. 2 (color online).   Equilibrium position of the microparticle as function of g^* together with a fourth-order fit through the data points.
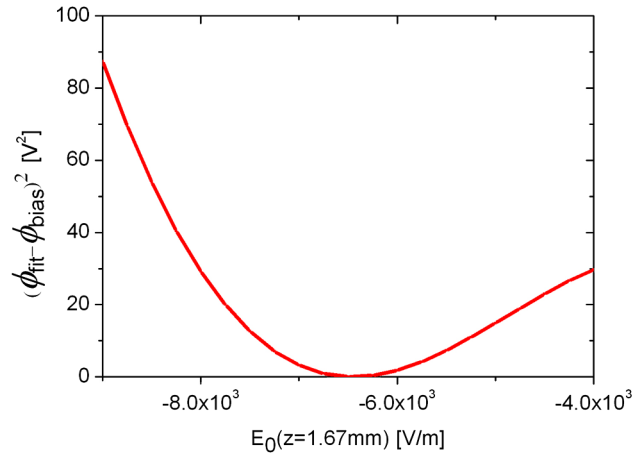
FIG. 3 (color online).   Deviation of the extrapolated electrode potential form the measured electrode bias potential.

4. RESULTS AND DISCUSSION.—Figure 1 shows CCD camera images of a confined microparticle, under several (hyper-)gravity conditions. In Fig. 2 the particle equilibrium height z_E is plotted as function of g^*. As can be observed, z_E shifts towards the bottom electrode when g^* is increased. To verify whether this method is nonintrusive, the equilibrium position of a layer of 10 microparticles is measured. The results show the same equilibrium height as was measured from one microparticle and, hence, it is concluded that within measurable significance, the presence of one microparticle does not influence the sheath. For $g^* > 2.7g_0$, no experimental data points are available since, at these high g^* levels, $\vec{F}_E$ is not able anymore to compensate for $\vec{F}_g$ and consequently the microparticle is lost to the electrode.

The function $g^*(z_E)$, to be used in Eq. (5), is obtained by a fourth-order polynomial fit through the data points in Fig. 2. The error function values of this fit indicate that the fitting function fits the experimental data very well. Using
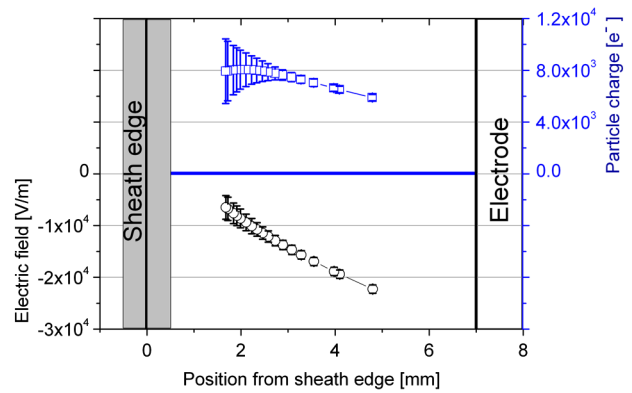
FIG. 4 (color online).   Obtained profiles for the electric field and the particle charge as function of the position in the sheath. The plotted error bars are mainly due to uncertainty in the Langmuir probe measurements.
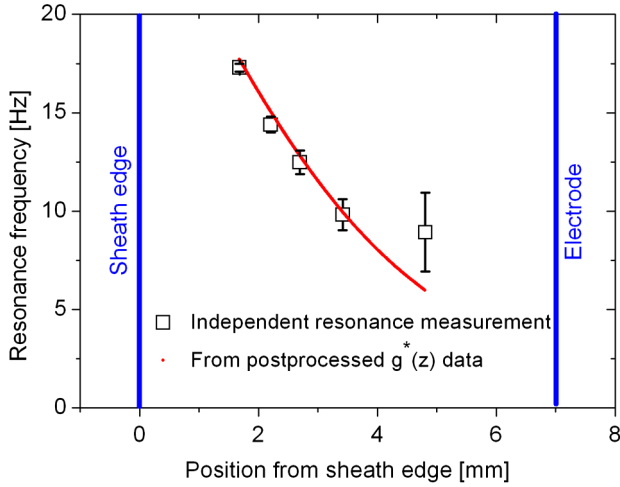
FIG. 5 (color online). Resonance frequency curve determined from the $E(z_E)$ and $Q_p(z_E)$ profiles in Fig. 4 compared with independently performed measurements of the microparticle's resonance frequency.

higher order fitting functions does not decrease the error function significantly. According to the procedure mentioned above for determining the best boundary condition, Fig. 3 shows the deviation of the extrapolated electrode potential from the measured electrode potential. From this figure, the best boundary condition at $z = 1.67$ mm appears to be $E_0 = -6485$ V/m.

The obtained $Q_p(z_E)$ and $E(z_E)$ profiles are presented in Fig. 4. The plotted error bars are mainly due to uncertainty in the Langmuir probe measurements. Both the shape and the absolute values of the $E(z_E)$ profile are in good agreement with profiles determined from sheath models presented by other researchers [9].

The error bars on the first few data points of the $Q_p(z_E)$ profile are too large to draw conclusions from. However, closer to the electrode, the particle charge decreases as function of z_E; i.e., from $(8 \pm 1) \times 10^3 e^-$ at $z_E = 2.2$ mm to $(5.9 \pm 0.3) \times 10^3 e^-$ at $z_E = 4.8$ mm.

In order to verify the method applied in this Letter, we have independently measured the resonance frequency of the microparticle at several particle equilibrium positions by applying a small ($< 2.5\%$) amplitude modulation to the rf power (see Refs. [8,10] for a description of the used method). With the CCD camera (with large exposure time), the maximum amplitude of the oscillating particle has been measured as function of the applied modulation frequency. For several equilibrium positions the frequency at which this amplitude is maximum is used as resonance frequency and is plotted in Fig. 5. The results are compared with the resonance curve calculated from the $Q_p(z_E)$ and $E(z_E)$ profiles presented in Fig. 4 via [10]

$$f_0(z) = \frac{1}{2\pi} \sqrt{\frac{1}{m_p} \left[Q_p(z_E) \frac{dE(z_E)}{dz_E} + E(z_E) \frac{dQ_p(z_E)}{dz_E} \right]}.$$

(6)

In Fig. 5 it can be observed that, except for one data point at high g^* of which the large error bar is due to vibrations induced by the centrifuge, the independently measured resonance frequencies show good agreement with the resonance curve obtained from the $Q_p(z_E)$ and $E(z_E)$. This indicates the validity and the strength of this method.

CONCLUSIONS.—In conclusion, we have obtained, by using microparticles as electrostatic probes under hypergravity conditions in a centrifuge, nonintrusively and without disturbing or changing plasma parameters both the electric field profile in the rf plasma sheath and the charge of the microparticle as function of position in the sheath. The obtained $E(z_E)$ profile shows good agreement with literature and, for $z_E > 2.2$ mm, the particle charge decreases for positions closer to the electrode.

[1] M. A. Lieberman, IEEE Trans. Plasma Sci. **17**, 338 (1989).
[2] V. A. Godyak and N. Sternberg, Phys. Rev. A **42**, 2299 (1990).
[3] T. E. Sheridan and J. Goree, Phys. Fluids B **3**, 2796 (1991).
[4] U. Czarnetzki, D. Luggenholscher, and H. F. Dobele, Plasma Sources Sci. Technol. **8**, 230 (1999).
[5] C. A. Moore, G. P. Davis, and R. A. Gottscho, Phys. Rev. Lett. **52** 538 (1984).
[6] E. Wagenaars, M. D. Bowden, and G. M. W. Kroesen, Phys. Rev. Lett. **98**, 075002 (2007).
[7] H. Yamada and D. L. Murphree, Phys. Fluids **14**, 1120 (1971).
[8] A. A. Samarian and B. W. James, Plasma Phys. Controlled Fusion **47**, B629 (2005).
[9] R. Basner et al., New J. Phys. **11**, 013041 (2009).
[10] C. Zafiu, A. Melzer, and A. Piel, Phys. Rev. E **63**, 066403 (2001).
[11] H. Kersten, R. Wiese, H. Neumann, R. Hipples, Plasma Phys. Controlled Fusion **48**, B105 (2006).
[12] S. Ratynskaia et al., Phys. Rev. Lett. **93**, 085001 (2004).
[13] R. Seurig et al., Acta Astronaut. **61**, 940 (2007).
[14] V. E. Fortov et al., Phys. Rep. **421** 1 (2005).
[15] M. A. Lieberman and A. J. Lichtenberg, *Principles of Plasma Discharges and Materials Processing* (John Wiley & Sons, New York, 1994).
[16] Z. Sternovsky and S. Robertson, IEEE Trans. Plasma Sci. **34**, 850 (2006).
[17] K. U. Riemann and P. Meyer, Phys. Plasmas **3**, 4751 (1996).